Single Phase Lock Loop

davide bagnara

December 11, 2025

Contents

List of Figures

List of Tables

1 Introduction

In this document the following topics are slightly covered:

- phase locked loop for single phase signals;
- moving average filter;
- discrete Fourier transform;
- Simulink C-caller;
- dSPACE SCALEXIO.

The idea of the document is to propose an laboratory application of a single-phase *PLL*, and moving average filter implemented in a fast prototyping equipment. The moving average filter will be implemented using customized C-code and Simulink C-caller.

2 Nomenclature

Here a list of symbols, variables, and parameters used along the document:

- *PLL*: phase locked loop;
- *VCO*: voltage controlled oscillator;
- *PI*: proportional integral controller;
- *LF*: loop filter;
- *PD*: phase detector;
- *SOGI*: second order generalized integrator;
- *QSG*: quadrature signal generator;
- *MAVG*: moving average;
- RMB: right mouse button;
- LMB: left mouse button;
- HMI: human machine interface;
- ConfigurationDesk: dSPACE application used to configure a project with the scalexio equipment;
- ControlDesk: dSPACE application used as HMI;
- $v,\ v_{signal}\quad \left[\mathrm{V}\right]$: input signals;
- $\alpha\beta$: direct and quadrature components of a vector quantity, generally with respect to a stationary reference frame;
- $\xi\eta$: additional direct and quadrature components of a vector quantity, generally with respect to a rotating reference frame;

3 Basic Structure of a Phase-Locked Loop

The basic structure of the phase-locked loop (*PLL*) is shown in Figure 1. It consists of three fundamental blocks:

- *phase detector* (*PD*). This block generates an output signal proportional to the phase difference between the input signal, v_{signal}, and the signal generated by the internal oscillator of the *PLL*, v^{pll}. Depending on the type of *PD*, high frequency AC components appear together with the DC phase-angle difference signal.
- *loop filter* (*LF*). This block presents a low pass filtering characteristic to attenuate the high frequency AC components from the PD output. Typically, this block is constituted by a first order low pass filter or a PI controller.
- *voltage controlled oscillator* (*VCO*). This block generates at its output an AC signal whose frequency is shifted with respect to a given central frequency, ω_{ff}, as a function of the input voltage provided by the *LF*.

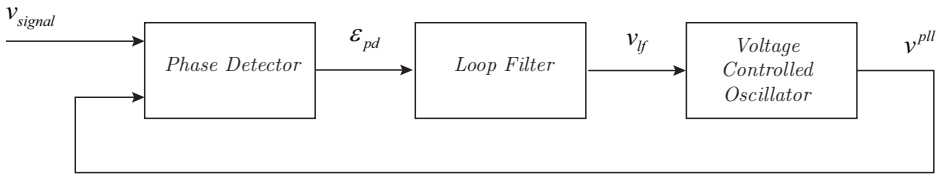

Figure 1: Basic structure of a PLL.

The block diagram of an elementary *PLL* is shown in Figure 2. In this case *PD* is implemented by means of the *Superheterodyne* technique, the *LF* is based on a *PI* controller and the *VCO* consists of a sinusoidal function supplied by a linear integrator.

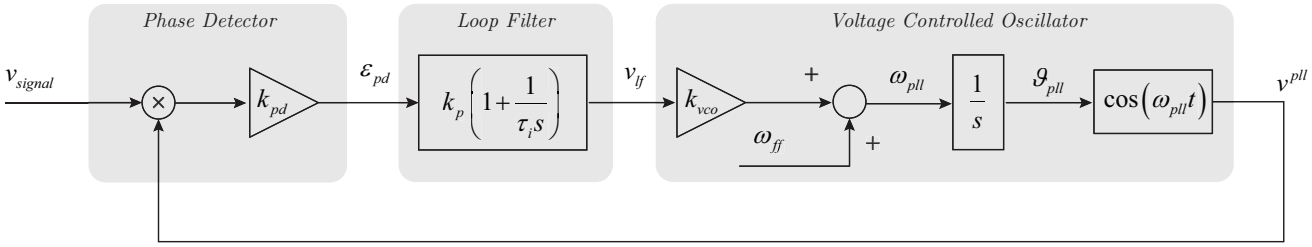

Figure 2: Block diagram of an elementary *PLL*.

If the input signal applied to this system is given by

$$v = V\sin(\vartheta) = V\sin(\omega t + \phi) \tag{3.1}$$

and the signal generated by the *VCO* is given by

$$v^{pll} = \cos(\vartheta_{pll}) = \cos(\omega_{pll}t + \phi_{pll}) \tag{3.2}$$

the phase error signal from the multiplier *PD* output can be written as

$$\begin{aligned}\varepsilon_{pd} &= Vk_{pd}\sin(\omega t + \phi)\cos(\omega_{pll}t + \phi_{pll}) \\ &= \frac{Vk_{pd}}{2}\Big[\sin[(\omega - \omega_{pll})t + (\phi - \phi_{pll})] + \sin[(\omega + \omega_{pll})t + (\phi + \phi_{pll})]\Big]\end{aligned} \tag{3.3}$$

The high frequency components $(\omega + \omega_{pll})$ of the *PD* error signal will be cancelled out by the *LF*, only the low frequency term $(\omega - \omega_{pll})$ will be processed, therefore, the *PD* error signal to be considered is

$$\varepsilon_{pd} = \frac{V k_{pd}}{2} \sin[(\omega - \omega_{pll})t + (\phi - \phi_{pll})] \tag{3.4}$$

If it is assumed that the *VCO* is well tuned to the input frequency, i.e. with $\omega \approx \omega_{pll}$, the DC term of the phase error is given as follows

$$\varepsilon_{pd} = \frac{V k_{pd}}{2} \sin(\phi - \phi_{pll}) \tag{3.5}$$

It can be observed in (3.5) that the multiplier *PD* produces nonlinear phase detection because of the sinusoidal function. However, when phase error is very small, i.e. when $\phi \approx \phi_{pll}$, the output of the multiplier *PD* can be linearized in the vicinity of such an operating point since $\sin(\phi - \phi_{pll}) \approx \sin(\vartheta - \vartheta_{pll}) \approx (\vartheta - \vartheta_{pll})$. Therefore, once the *PLL* is locked, the relevant term of the phase error signal is given by

$$\varepsilon_{pd} = \frac{V k_{pd}}{2} (\vartheta - \vartheta pll) \tag{3.6}$$

According to Eq. (3.6), the model presented in Figure 2 can be linearized around the condition of $\omega \approx \omega_{pll}$ resulting as per Figure 3.

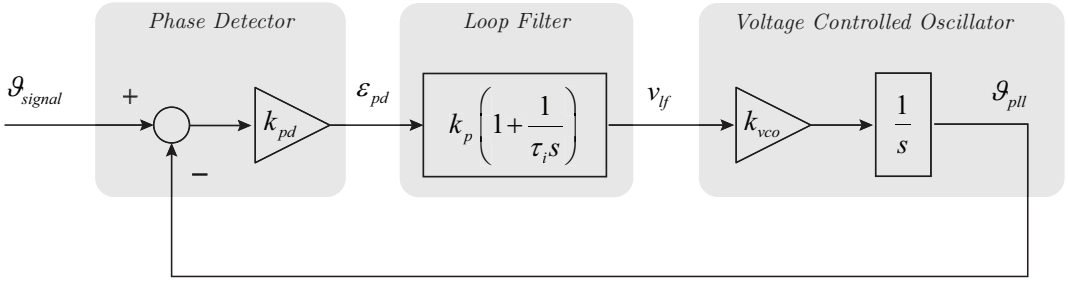

Figure 3: Small signal model of an elementary *PLL*.

According to the block diagram of Figure 3 a frequency domain analysis brings to the following transfer functions (consider $k_{pd} = k_{vco} = 1$):

$$H(s) = PD(s)LF(s)VCO(s) = \frac{k_p s + \frac{k_p}{\tau_i}}{s^2} \tag{3.7}$$

$$H_\vartheta(s) = \frac{\Theta_{pll}(s)}{\Theta(s)} = \frac{H(s)}{1 + H(s)} = \frac{k_p s + \frac{k_p}{\tau_i}}{s^2 + k_p s + \frac{k_p}{\tau_i}} \tag{3.8}$$

$$E_\vartheta = \frac{E_{pd}(s)}{\Theta(s)} = 1 - H_\vartheta(s) = \frac{s^2}{s^2 + k_p s + \frac{k_p}{\tau_i}} \tag{3.9}$$

The open loop transfer function of Eq. (3.7) shows that the *PLL* has two poles at the origin, which means that is able to track even a constant slope ramp in the input phase angle without any steady state error.

4 SOGI-QSG-based PLL

Figure 4 shows the structure of a *VCO* based on *QSG*; the structure consists of an adaptive filter.

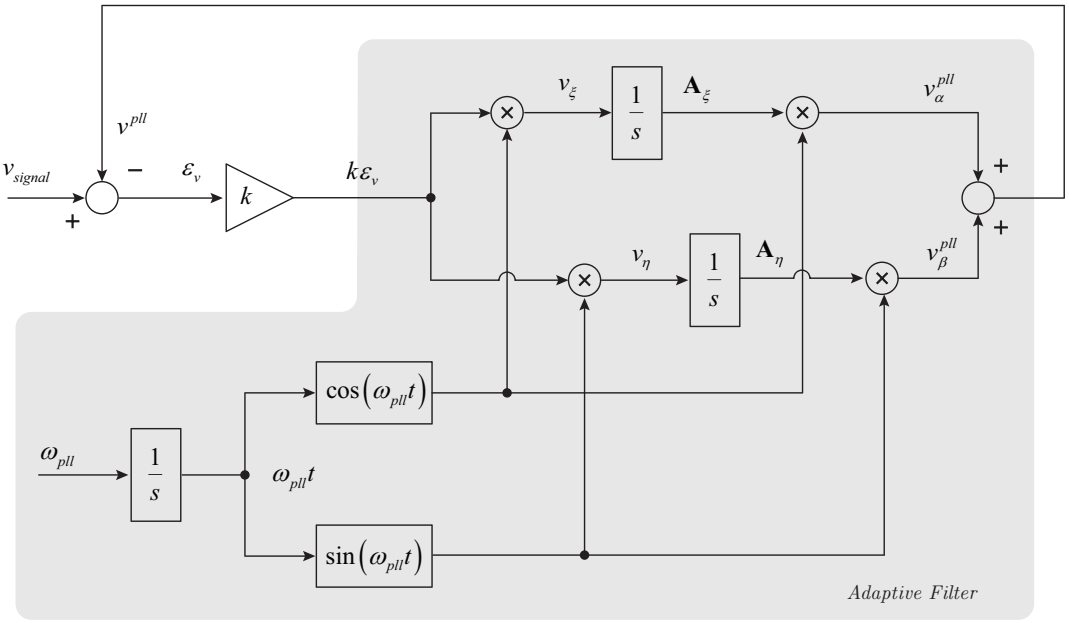

Figure 4: Voltage controlled oscillator based on a adaptive filter.

Defining $g = k\epsilon_v$, the v_ξ, and v_η components of Figure 4 can be written as follows

$$v_\xi = g\cos(\omega_{pll}) = \frac{1}{2}g\Big(e^{j\omega_{pll}t} + e^{-j\omega_{pll}t}\Big) \tag{4.1}$$

$$v_\eta = g\cos(\omega_{pll}) = -j\frac{1}{2}g\Big(e^{j\omega_{pll}t} - e^{-j\omega_{pll}t}\Big) \tag{4.2}$$

The $\mathbf{A}_\xi$, and $\mathbf{A}_\eta$ terms which correspond to the output of the integrators for v_ξ and v_η, can be expressed in the Laplace domain as follows

$$\mathbf{A}_\xi = \frac{1}{s}v_\xi(s) = \frac{1}{2s}\Big[g(s+j\omega_{pll}t) + g(s-j\omega_{pll}t)\Big] \tag{4.3}$$

$$\mathbf{A}_\eta = \frac{1}{s}v_\eta(s) = -j\frac{1}{2s}\Big[g(s+j\omega_{pll}t) - g(s-j\omega_{pll}t)\Big] \tag{4.4}$$

and the v_α^{pll}, v_β^{pll} terms result as follows

$$\begin{aligned} v_\alpha^{pll} &= \frac{1}{2}\Big[\mathbf{A}_\xi(s+j\omega_{pll}t) + \mathbf{A}_\xi(s-j\omega_{pll}t)\Big] \\ &= \frac{1}{4(s+j\omega_{pll})}\Big[g(s) + g(s+j\omega_{pll}t)\Big] + \frac{1}{4(s-j\omega_{pll})}\Big[g(s) + g(s-j\omega_{pll}t)\Big] \end{aligned} \tag{4.5}$$

$$\begin{aligned} v_\beta^{pll} &= -j\frac{1}{2}\Big[\mathbf{A}_\xi(s+j\omega_{pll}t) - \mathbf{A}_\xi(s-j\omega_{pll}t)\Big] \\ &= \frac{1}{4(s+j\omega_{pll})}\Big[g(s) + g(s+2j\omega_{pll}t)\Big] + \frac{1}{4(s-j\omega_{pll})}\Big[g(s) - g(s-2j\omega_{pll}t)\Big] \end{aligned} \tag{4.6}$$

The term $v^{pll} = v_\alpha^{pll} + v_\beta^{pll}$ results as follows

$$v^{pll} = v_\alpha^{pll} + v_\beta^{pll} = \frac{s}{s^2+\omega_{pll}^2}g(s) \tag{4.7}$$

Consequently, the transfer functions of the adaptive filter *VCO* structure of Figure 4 are given by

$$\frac{v^{pll}}{\varepsilon_v}(s) = \frac{ks}{s^2 + \omega_{pll}^2} \tag{4.8}$$

$$\frac{v^{pll}}{v}(s) = \frac{ks}{s^2 + ks + \omega_{pll}^2} \tag{4.9}$$

$$\frac{\varepsilon_v}{v}(s) = \frac{s^2 + \omega_{pll}^2}{s^2 + ks + \omega_{pll}^2} \tag{4.10}$$

The structure of Figure 4 can be used of quadrature signal generator (*QSG*) by adding a scaled integrator at the output of the adaptive filter, as in Figure 5 is shown.

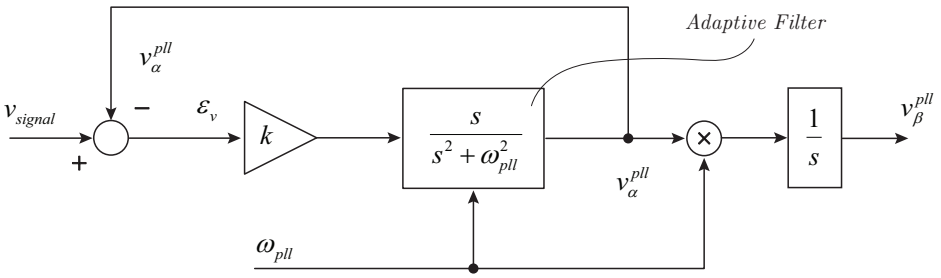

Figure 5: Quadrature signal generator based on a adaptive filter.

Clearly, the response of the AF block, shown in Figure 4 is defined by Eq. (4.8) in the case of applying a likewise sinusoidal signal (sine or cosine) with frequency ω_{pll} to its input.

Recalling that

$$\mathscr{L}\Big[\sin(\omega_{pll})\Big] = \frac{\omega_{pll}}{s^2 + \omega_{pll}^2} \tag{4.11}$$

$$\mathscr{L}\Big[\cos(\omega_{pll})\Big] = \frac{s}{s^2 + \omega_{pll}^2} \tag{4.12}$$

the time response of the system characterized by Eq. (4.8) in the presence of sinusoidal inputs is given by

$$\mathscr{L}^{-1}\left[\frac{\omega_{pll}}{s^2 + \omega_{pll}^2}\frac{s}{s^2 + \omega_{pll}^2}\right] = \frac{1}{2}t\sin(\omega_{pll}t) \tag{4.13}$$

and

$$\mathscr{L}^{-1}\left[\frac{s}{s^2 + \omega_{pll}^2}\frac{s}{s^2 + \omega_{pll}^2}\right] = \frac{1}{2}\left[\frac{\sin(\omega_{pll}t)}{\omega_{pll}} + t\cos(\omega_{pll}t)\right] \approx \frac{1}{2}t\cos(\omega_{pll}t) \tag{4.14}$$

An efficient implementation of the structure of Figure 5 is shown in Figure 6, where

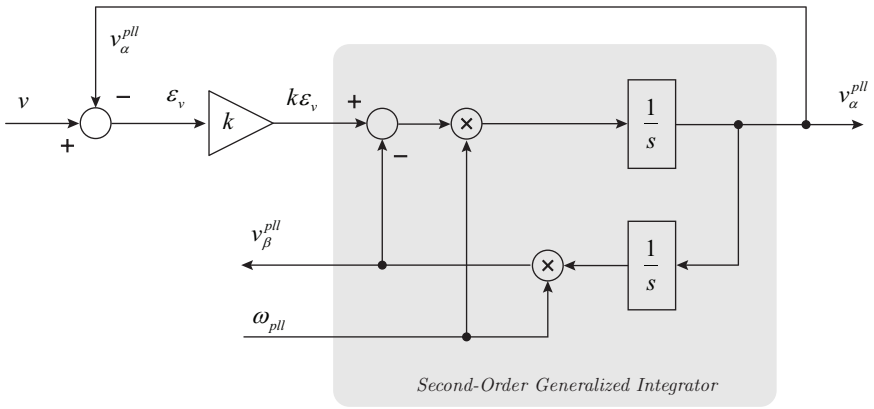

Figure 6: Second order adaptive filter based on an second order generalized integrator and a quadrature signal generator (*SOGI-QSG*).

$$SOGI(s) = \frac{v_\alpha^{pll}}{\varepsilon_v}(s) = \frac{k\,\omega_{pll}\,s}{s^2 + \omega_{pll}^2} \tag{4.15}$$

$$D(s) = \frac{v_\alpha^{pll}}{v}(s) = \frac{k\,\omega_{pll}\,s}{s^2 + k\,\omega_{pll}\,s + \omega_{pll}^2} \tag{4.16}$$

$$Q(s) = \frac{v_\beta^{pll}}{v}(s) = \frac{k\,\omega_{pll}^2}{s^2 + k\,\omega_{pll}\,s + \omega_{pll}^2} \tag{4.17}$$

Based on the structure of the *SOGI-QSG* of Figure 6 it is possible to implement a *SOGI-QSG*-based *PLL* as shown in Figure 7.

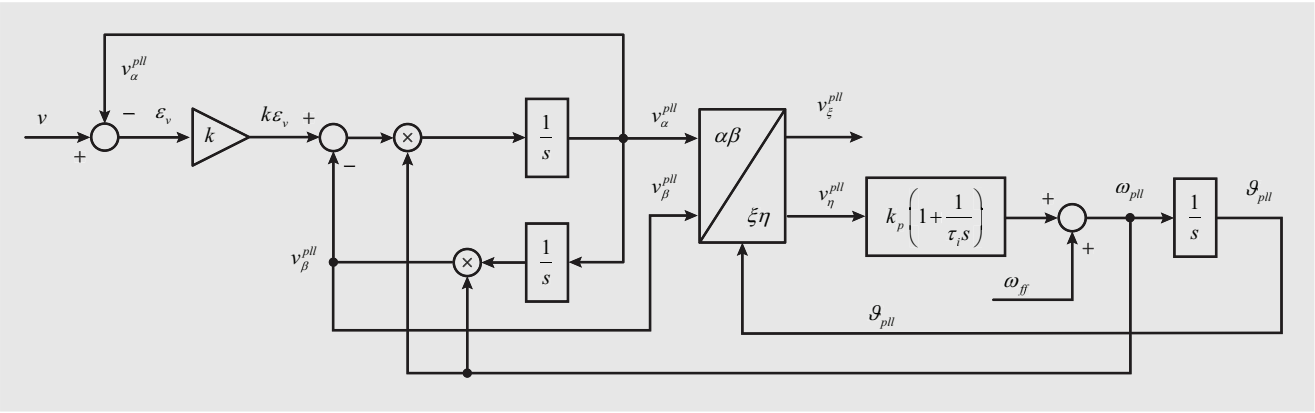

Figure 7: Diagram of the *SOGI*-based *PLL* (*SOGI-QSG*).

The transfer function from the input signal v to the error signal ε_v is given by

$$E(s) = \frac{\varepsilon_v}{v}(s) = \frac{s^2 + \omega_{pll}^2}{s^2 + k\,\omega_{pll}\,s + \omega_{pll}^2} \tag{4.18}$$

The transfer function of Eq. (4.18) responds to a second order notch filter, with zero gain at the centre frequency (ω_{pll}).

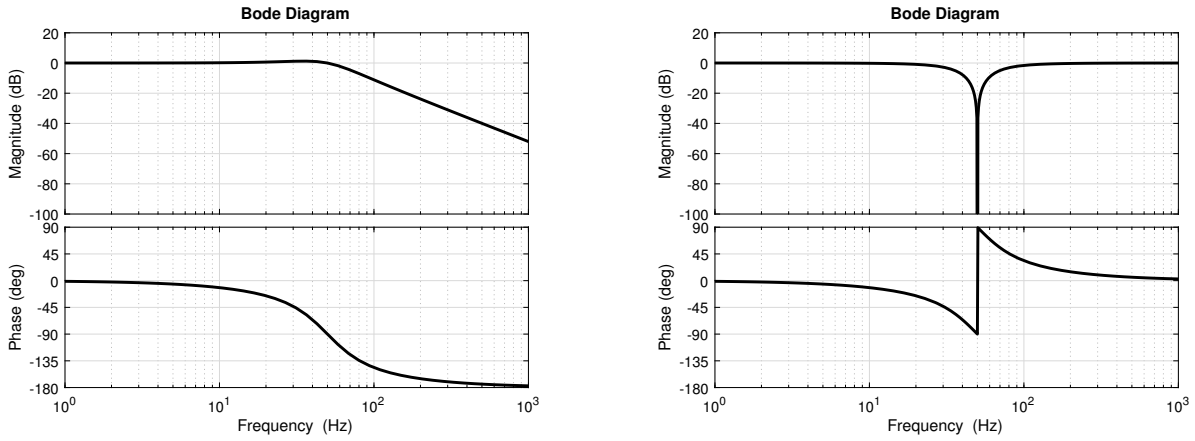

(a) Bode diagram of the $Q(s)$ transfer function in a *SOGI-QSG*.

(b) Bode diagram of the $E(s)$ transfer function in a *SOGI-QSG*.

Figure 8: Bode diagram of the *SOGI-QSG* response.

Another useful possible implementation of the *SOGI-QSG*-based *PLL* is based on the direct and inverse Park transforms, as shown in Figure 9

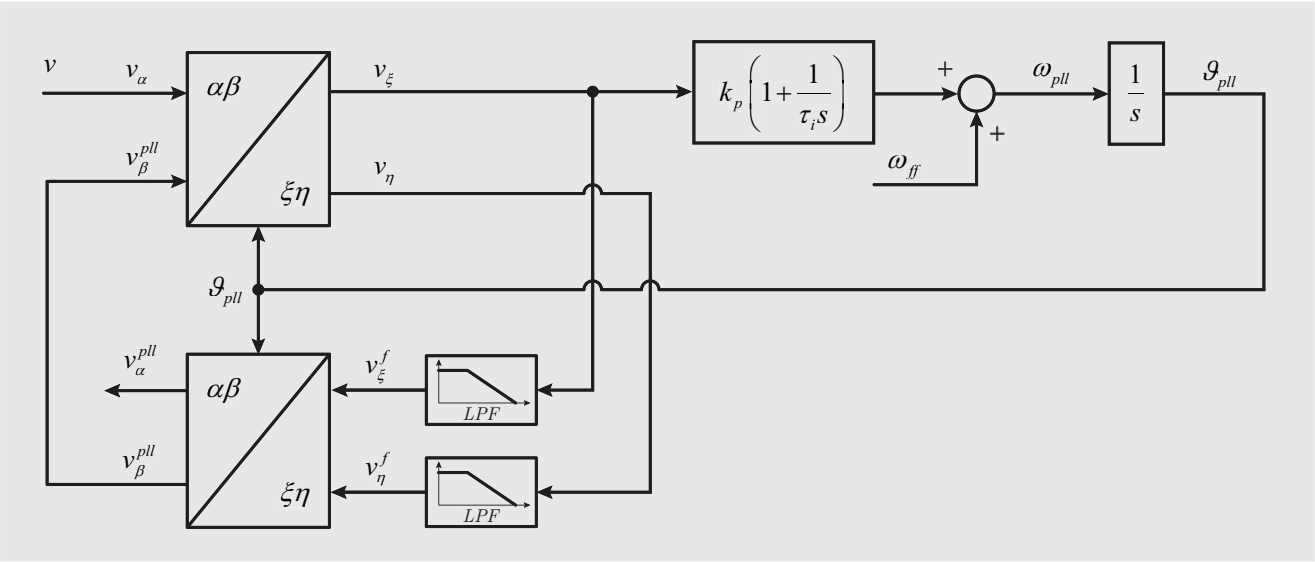

Figure 9: PLL based on the on direct and inverse Park transform.

An equivalent transfer function block diagram is presented in Figure 10. In this configuration the transformation $v_\alpha \rightarrow v_\beta^{pll}$ is represented as ω_{pll}/s in Laplace domain. An intuitive explanation of its operation principle can be given if it is assumed that the *PLL* is well tuned to the input signal frequency. Under such operation conditions, if v_α and v_β^{pll} are not in quadrature, the virtual input vector, v_α^{pll}, resulting from these signals will have neither constant amplitude nor rotation speed.

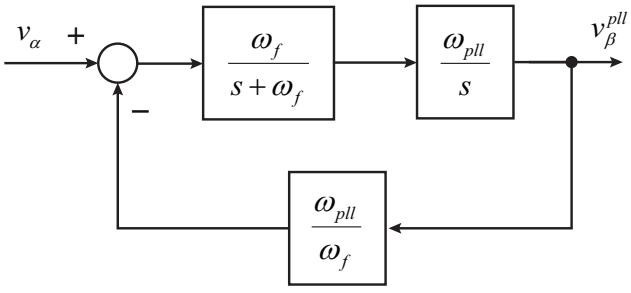

Figure 10: Equivalent block diagram of the PLL based on the on direct and inverse Park transform.

Therefore v_ξ and v_η waveform resulting from direct Park transformation will have harmonics components. These harmonics will be suppressed by the *LPF* blocks generating, as well, the components v_ξ^f and v_η^f. The v_α and v_β^{pll} components resulting from the inverse Park transformation of the components v_ξ^f and v_η^f will be in quadrature, though v_α and v_α^{pll} will not be in phase if the *PLL* is not perfectly synchronized. As the *PLL* locks the phase angle of the input signal v_α, the components v_α^{pll} and v_β^{pll} will be respectively in phase and in quadrature respect to the input signal v_α.

From the equivalent block diagram of Figure 10 the following transfer functions can be derived

$$\boxed{\frac{V_\beta^{pll}}{V_\alpha}(s) = \frac{\omega_f \omega_{pll}}{s^2 + \omega_f s + \omega_{pll}^2}} \tag{4.19}$$

$$\boxed{\frac{V_\alpha^{pll}}{V_\alpha}(s) = \frac{s\omega_f}{s^2 + \omega_f s + \omega_{pll}^2}} \tag{4.20}$$

where the relation of Eq. (4.21) has been applied.

$$V_\beta^{pll}(s) = \frac{\omega_{pll}}{s} V_\alpha^{pll}(s) \tag{4.21}$$

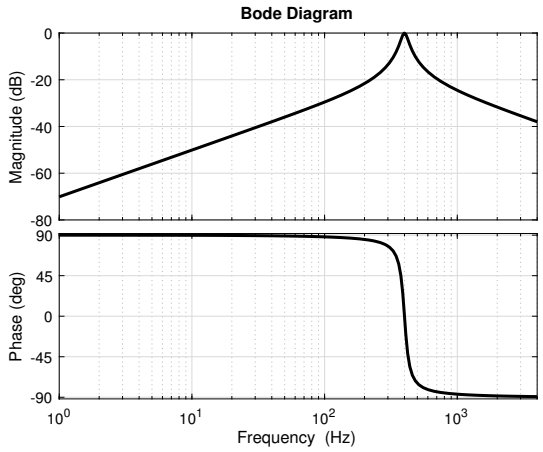

(a) Bode diagram of the $\frac{V_\alpha^{pll}}{V_\alpha}(s)$ transfer function, with $\omega_f = 2\pi 50\,\text{Hz}$, and $\omega_{pll} = 2\pi 400\,\text{Hz}$.

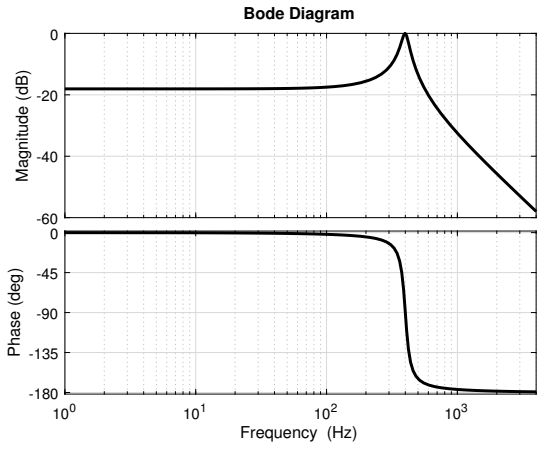

(b) Bode diagram of the $\frac{V_\beta^{pll}}{V_\alpha}(s)$ transfer function, with $\omega_f = 2\pi 50\,\text{Hz}$, and $\omega_{pll} = 2\pi 400\,\text{Hz}$.

Figure 11: Bode diagram of the *QSG-PLL* based on direct and inverse Parck transform.

References

[1] R. Teodorescu, M. Liserre, P. Rodrıguez, *Grid converters for photovoltaic and wind power systems.* Wiley, 2011.